
Proceedings Paper:
Angelides, S., Burgan, B., Kyprianou, C. et al. (2023) An application of the Hudson clearing method to near-field blast loading and above-ground explosions. In: Proceedings of the 6th International Conference on Protective Structures (ICPS6). 6th International Conference on Protective Structures (ICPS6), 14-17 May 2023, Auburn, AL, United States. International Association of Protective Structures.

6th International Conference on Protective Structures (ICPS6)
14 – 17 May 2023, Auburn University USA

AN APPLICATION OF THE HUDSON CLEARING METHOD TO NEAR-FIELD BLAST LOADING AND ABOVE-GROUND EXPLOSIONS

Socrates C. Angelides
Dr, Steel Construction Institute / University of Sheffield, Silwood Park, Ascot, Berkshire, SL5 7QN, UK, s.angelides@steel-sci.com (corresponding author)

Bassam A. Burgan and Constantinos Kyprianou
Dr and Dr, Steel Construction Institute, Silwood Park, Ascot, Berkshire, SL5 7QN, UK.

Samuel E. Rigby and Andrew Tyas
Dr and Prof, University of Sheffield, Department of Civil and Structural Engineering, Mappin Street, Sheffield, S1 3JD, UK.

ABSTRACT
Clearing effects influence the pressure-time history experienced by surface structures of finite size. This is a phenomenon that results in gradually reducing the reflected pressures on the front face of a building, to the lower free-field pressures experienced by the sides and roof. The Hudson method is a first-principles approach to account for clearing effects on finite surface structures by superimposing the reflected pressures derived on infinite surfaces with pressure relief waveforms travelling from the free edges. This method has shown good agreement with experimental and numerical results in the mid- and far-field, when a single Friedlander blast wave is assumed to impinge on a surface. This paper will explore the application of the Hudson clearing method to above-ground explosions with targets located above the triple-point path, where the pulse consists of two Friedlander blast waves, resulting from the incident and ground-reflected waves arriving separately at the target. Furthermore, the limitations of the Hudson clearing method to near-field explosions will also be assessed. For both cases, the semi-empirical Low Altitude Multiple Burst (LAMB) addition method will be considered in the derivation of the reflected pressure-time histories on infinite surfaces. To assess the predictions of the Hudson clearing method, these will be compared with the results from computational fluid dynamic analyses.

Keywords: Blast loading, clearing, near-field, triple-point path

INTRODUCTION

The free-field and reflected pressure-time histories at a target location, resulting from the detonation of high-explosives, can be predicted empirically by deriving the key blast parameters (peak pressure, impulse, time of arrival and duration) and defining the shape of the pulse. The former can be derived from polynomial equations that have been fitted to blast trials (Kingery and Bulmash 1984). These equations have been implemented in military standards and are included in the appendix of UFC 3-340-01 and presented in the form of graphs in UFC 3-340-02. For design purposes, the latter is often approximated as a right triangular pressure-time history, where the positive phase is represented as a linearly decaying straight line (UFC 3-340-02). Alternatively, more refined pulse shapes can be assumed for the positive and negative phase of the free-field blast loading, such as the modified Friedlander equation and cubic expression, respectively. Subsequently, the reflected blast loading on an infinite surface can be derived from the Low Altitude Multiple Burst (LAMB) addition of the free-field (i.e. incident) and target-reflected waves. This is a semi-empirical method that is implemented in the EMBlast software, where the target-reflected waves are assumed to originate from a fictitious charge (image) of identical weight and located symmetrically to the actual charge (real), with respect to the target surface (Angelides et al. 2022).

Clearing effects influence the pressure-time history experienced by surface structures of finite size. This is a phenomenon that results in gradually reducing the reflected pressures on the front face of a building, to the lower free-field pressures experienced by the sides and roof. UFC 3-340-02 includes an empirical equation for calculating the ‘‘clearing time’’, i.e. the duration over which the reflected pressure linearly decays to the stagnation pressure. However, a comparison with numerical results has demonstrated that the UFC predictive clearing method is only valid for targets of scaled height $Z/250$ and smaller, where $Z = R/W^{1/3}$ is the scaled distance, R is the standoff distance between the charge and the target, and W is the charge weight. This limitation is most likely attributed to the derivation of the empirical ‘‘clearing time’’ equation from large-scale high-explosive and nuclear tests, where the reflecting surfaces considered were 2-3 orders of magnitude smaller compared to the standoff distance (Rigby et al. 2015a). Furthermore, the UFC predictive method is limited to the positive phase of the blast loading, and can only be applied when this is represented as a straight line.

The Hudson clearing method offers an alternative, first-principles approach for predicting clearing effects, by superimposing the reflected pressure-time history derived for an infinite target surface with pressure relief waveforms travelling from the edge of a finite target surface. Hudson (1955) derived pressure relief waveforms using the Sommerfeld diffraction theory and presented these in graphical form as a function of a nondimensional length $\eta = x/\lambda$, where x is the distance of the target point to the nearest free edge and λ is the spatial length of the positive phase of the incident Friedlander pulse (can be derived as the product of the acoustic wave speed times the positive phase duration). The de-classification of Hudson’s work in 1998 led to the recent research interest in validating Hudson’s clearing method with experimental results and computational fluid dynamic (CFD) simulations (Tyas et al. 2011, Rigby 2014, Rigby et al. 2015a). Compared to the UFC clearing method, the Hudson method accounts for clearing effects for both the positive and negative phase of the blast loading. Furthermore, this method has no limitation with regards to the scaled height of the target, with the Hudson method predicting within 5% the specific impulse recorded experimentally for targets with scaled heights between $Z/28$ and $Z/11$ (Tyas et al. 2011). Finally, the Hudson method is not restricted to linearly idealised pulse shapes and can be combined with Friedlander blast waves. Therefore, this allows the superimposition of the pressure relief clearing waves with the reflected pressure-time histories derived from LAMB addition. The Hudson method could potentially also be combined with pulse shapes consisting of multiple Friedlander blast waves, such as the case of above-

ground explosions with targets located above the triple-point path, where the incident and ground-reflected waves arrive separately at the target, as shown in Figure 1. However, the application of the Hudson method to such pulses has not been previously investigated.

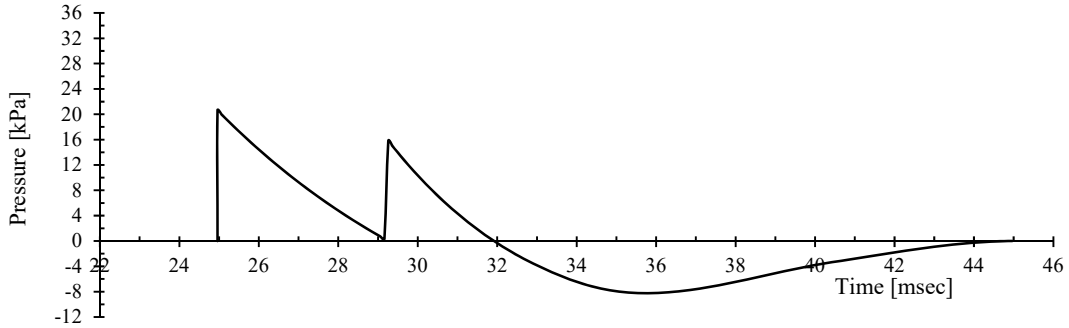

Figure 1. Pressure-time history generated by EMBlast for an above-ground explosion (W = 1 kg and R = 10.81 m) at a target point located 6.1 m above the ground.

Nartu et al. (2022) demonstrated that the predictions of the Hudson clearing method can be improved in the near-field by modifying the clearing wave speed in the calculation of the spatial length of the positive phase of the incident Friedlander pulse. Therefore, instead of using the ambient sound speed as a constant clearing wave speed, Nartu et al. proposed to use a variable clearing speed with respect to scaled distance that was derived analytically as a function of the reflected pressure-time history on an infinite surface using the relations of the speed of sound in air, thermodynamic relations and kinematics. For scaled distances greater than 2 m/kg$^{1/3}$, Nartu et al. demonstrated a good agreement of the derived analytical equation for the variable clearing speed with CFD results. Shin and Whittaker (2019), who performed multiple CFD simulations with Autodyn on infinite and finite surfaces for various scaled distances in the near-field ranging from 0.2 to 5 m/kg$^{1/3}$, also confirmed the variability of the clearing wave speed with scaled distance. Furthermore, Shin and Whittaker concluded that within the fireball radius, typically for scaled distances less than 0.8 m/kg$^{1/3}$, simplified right triangular or Friedlander pressure-time histories for the reflected blast wave on an infinite surface can no longer be assumed, as the pulse shape is affected from the expanding detonation products. This has also been experimentally observed by Rigby et al. (2015b), suggesting the limitation of applying the Hudson methodology to scaled distances less than 0.8 m/kg$^{1/3}$, as a Friedlander blast wave impinging normally on a finite surface has been assumed by Hudson (1995) in the derivation of the pressure relief waveforms.

This paper will discuss the combination of the semi-empirical LAMB addition method with the Hudson method for predicting the clearing effects on finite surface structures, hereafter referred to collectively as the EMBlast method, as this methodology is implemented in the aforementioned blast loading predictive software. The focus will be on above-ground explosions with targets located above the triple-point path and near-field blast loading with scaled distances greater than 0.8 m/kg$^{1/3}$. CFD simulations are performed and the results compared with the predictions of the EMBlast method.

ABOVE-GROUND EXPLOSIONS WITH TARGETS ABOVE THE TRIPLE-POINT PATH

In above-ground explosions, where a charge is located at a vertical distance from the ground (V_E), there are two reflection regimes in the space surrounding a target point. This depends whether the target is below or

above the triple-point path, defined as the collection of points along the normal distance from the charge to the target point (H), where the incident and ground-reflected waves intersect, as shown in Figure 2. When the target is located above the triple-point path, the incident and ground-reflected waves arrive separately at the target point. For such cases, the free-field pressure-time history in EMBlast is derived from the LAMB addition of the two waves, assuming that a ground-reflected wave is created by a fictitious (image) charge of identical weight to the actual (real) charge and located below the ground at the same distance as the actual charge above the ground (Angelides et al. 2022).

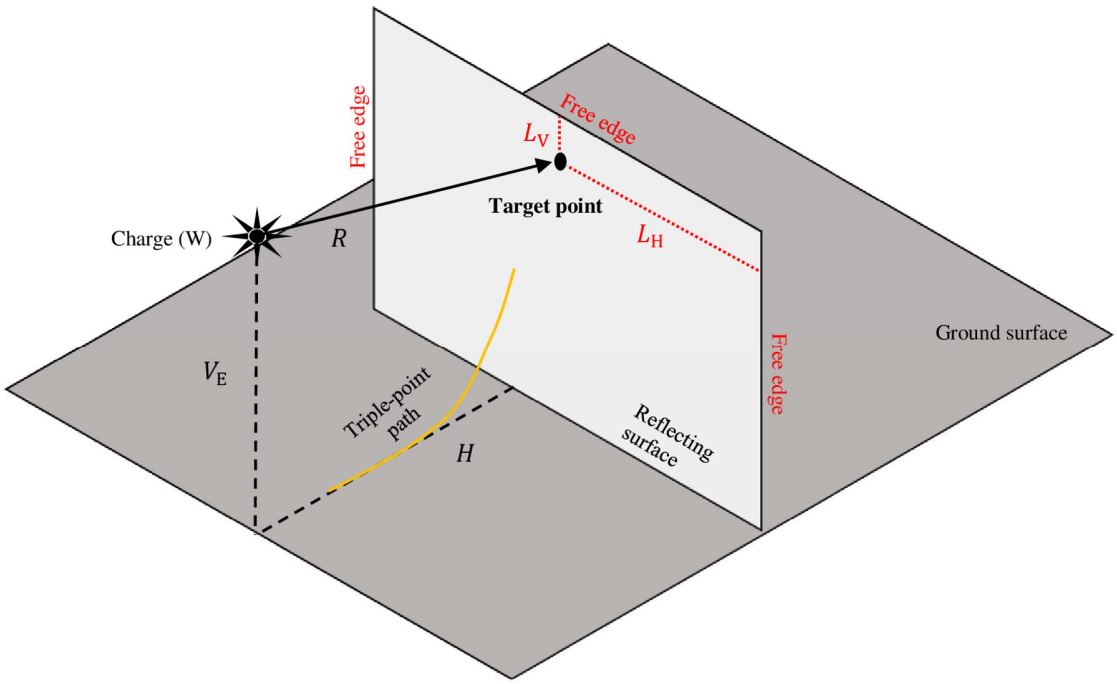

Figure 2. Sketch of an above-ground explosion with target located above the triple-point path indicating the distances of the target point to the nearest free edges.

To apply the Hudson methodology to finite surfaces with targets above the triple-point path, the vertical (L_V) and horizontal (L_H) distances from the target point to the nearest free edges need to be first defined, as shown in Figure 2. Pressure relief waveforms originating from each edge are then derived from Hudson's (1955) graphs, using the clearing wave speed modification proposed by Nartu et al. (2022). For above-ground explosions with target points below the triple-point path (also for free-air and surface explosions), a single pressure relief waveform is derived for each free edge. However, for above-ground explosions with target points above the triple-point path, two pressure relief waveforms are derived for each free edge to account separately for the clearing effects on the incident and ground-reflected waves. Figure 3 demonstrates the process for deriving the pressure-time history in EMBlast for a target point above the triple-point path that is located near the top of the finite surface, but far away from the sides ($L_V << L_H$) and therefore the clearing waves from the sides are ignored: first, the reflected pressure-time history on an infinite surface is derived using LAMB addition (Figure 3a); subsequently, two pressure relief waveforms originating from the top are derived from Hudson's (1955) graphs corresponding to the incident (Figure 3b) and the ground-reflected waves (Figure 3c); finally, the pressure-time history at the target point is derived by superimposing the reflected wave on an infinite surface and the two clearing waves (Figure 3d).

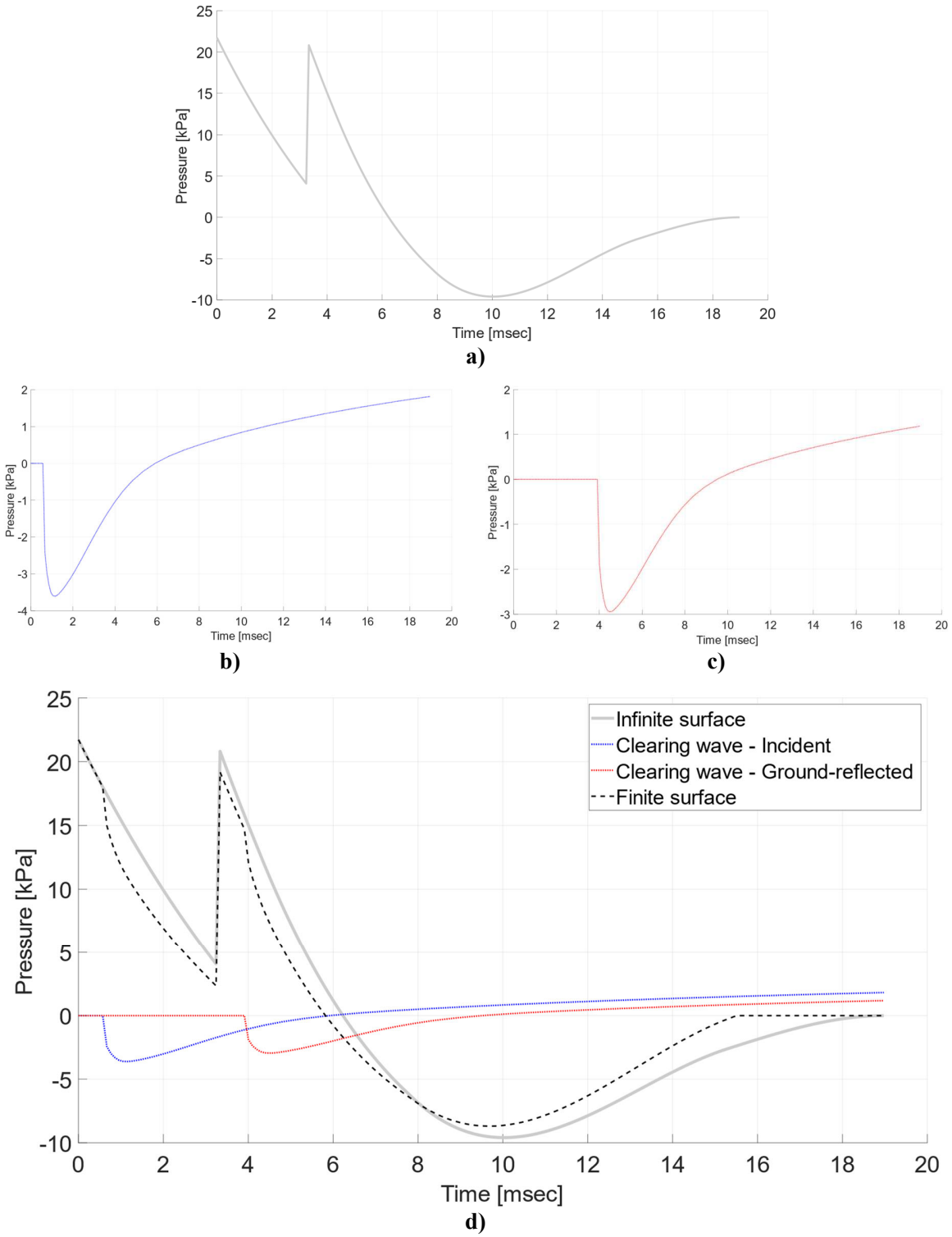

Figure 3. Above-ground explosion with target located above the triple-point path: a) reflected pressure-time history for an infinite surface, b) pressure-relief clearing wave for incident blast wave, c) pressure-relief clearing wave for ground-reflected blast wave and d) pressure-time history for a finite surface accounting for clearing effects.

NUMERICAL MODELS

CFD analyses are performed using BlastFoam to compare the predictions of the EMBlast method in the near-field and for above-ground explosions with targets above the triple-point path. Six three-dimensional (3D) quarter model analyses were performed at a scaled distance of 1.6 m/kg$^{1/3}$, considering a 1 kg Trinitrotoluene (TNT) charge of 1,630 kg/m^3 density at a standoff distance of 1.6 m to a reflecting surface. The Jones-Wilkins-Lee equation of state was used for TNT and the ideal gas equation of state for the air. In the first three models, a free-air explosion was modelled with the charge placed at the ground level, considering an infinite reflecting surface and finite reflecting surfaces of half widths, S, where S = 200 mm and 100 mm, respectively, as shown in Figure 4a. A coarse mesh of 100 mm was considered for the air along the standoff distance and a finer mesh of 12.5 mm for the charge, including five additional fine buffer cells between the charge and the air domain. For all three models, the pressure-time history was recorded at a monitor point (A) placed on the ground and at the middle of the reflecting surface ($L_v >> L_H$), corresponding to $L_{H,A}$ = 200 mm and 100 mm for the finite surface models of S = 200 mm and 100 mm, respectively. Furthermore, an additional monitor point (B) at the ground was placed for the finite surface models at a horizontal distance $L_{H,B}$ = 100 mm and 50 mm from the free edge for the S = 200 mm and 100 mm models, respectively. To validate the free-air explosion BlastFoam models, the pressure-time histories recorded at the middle of the reflecting surface were compared with the digitised graphs presented by Shin and Whittaker (2019), as shown in Figure 5, indicating a good agreement for all three models. Shin and Whittaker performed CFD analyses in Autodyn with a more refined mesh, considering one-dimensional (1D) domains of 1.6 mm cell size for both the air and the charge. The 1D results were subsequently mapped into a 3D domain of 10 mm cell size. Shin and Whittaker also performed CFD analyses for smaller scaled distances corresponding to 0.8 m/kg$^{1/3}$ and 1.0 m/kg$^{1/3}$, presenting pressure-time history graphs recorded at the middle of the reflecting surface. These analyses were not repeated with BlastFoam, however the digitised graphs were used to further validate the EMBlast method in the near-field.

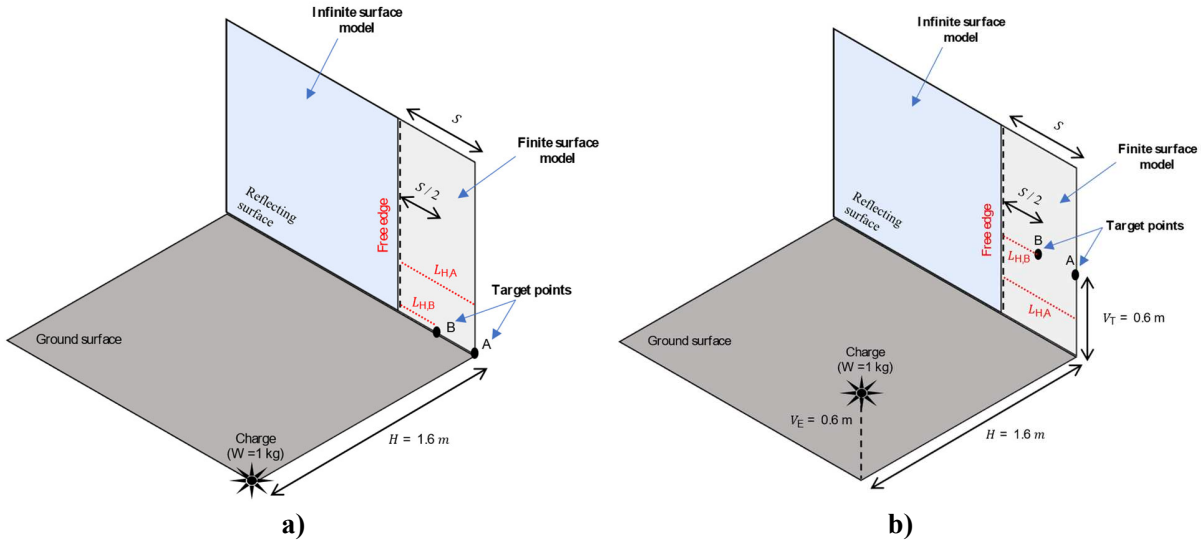

a) **b)**

Figure 4. Sketch indicating the six BlastFoam models considered: a) free-air explosion, b) above-ground explosion.

For the above-ground explosions, three additional analyses were performed, using the same parameters as the free-air explosions models, but the charge was placed at a vertical distance (V_E) of 0.6 m above the

ground, as shown in Figure 4b. The pressure-time histories were recorded at monitor points on the reflected surface at a vertical distance (V_T) of 0.6 m above the ground. This ensured the target points were above the triple-point path that is located at 0.4 m above the ground, as calculated from Figure 2.13 of UFC 3-340-02 at a scaled distance of 1.6 m/kg$^{1/3}$ for an above-ground explosion with scaled height of 0.6 m/kg$^{1/3}$.

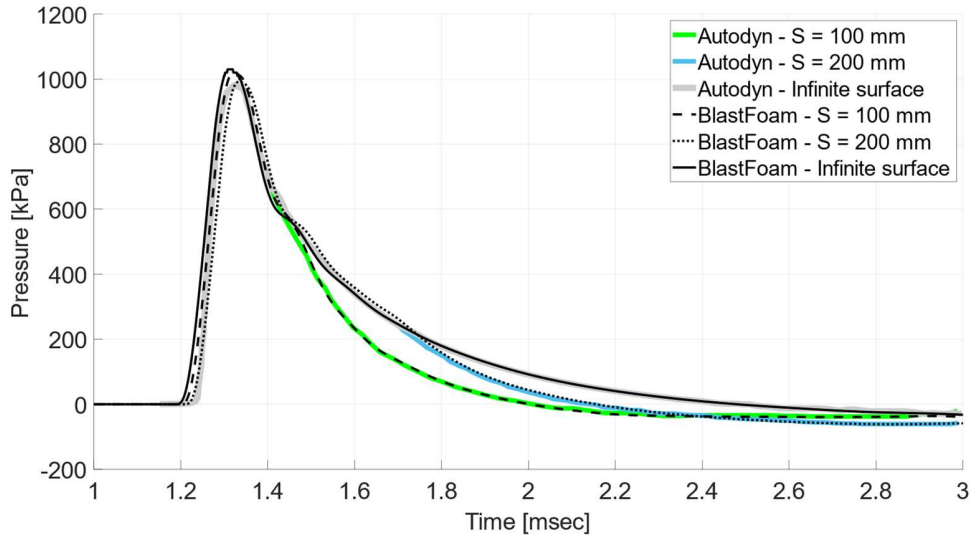

Figure 5. Comparison of free-air explosion (Z = 1.6 m/kg$^{1/3}$) pressure-time histories derived from BlastFoam with digitised values from Autodyn (Shin and Whittaker 2019) for an infinite surface and finite surfaces of half widths of S = 100 mm and 200 mm.

RESULTS AND DISCUSSION

Table 1 compares impulse values derived using the EMBlast method with results from CFD simulations (BlastFoam and Autodyn) for near-field free-air explosions. Three scaled distances are considered, 0.8 m/kg$^{1/3}$, 1.0 m/kg$^{1/3}$ and 1.6 m/kg$^{1/3}$. For the former two scaled distances, the CFD impulse values were derived by integrating the digitised graphs presented by Shin and Whittaker (2019). In most cases, the EMBlast method is overpredicting the CFD impulse values for finite surfaces, demonstrating a fast and conservative method for predicting clearing effects in the near-field for scaled distance greater than 0.8 m/kg$^{1/3}$. The overpredicted impulses are a consequence of the LAMB predictions for the reflected pressure-time history on infinite surfaces, and not due to the Hudson clearing predictions, as shown in the first row in Table 1. This is further highlighted in Figure 6 that compares the predicted EMBlast pressure-time histories on a finite surface of half-width equal to S = 100 mm with the BlastFoam results. The reflected pressure-time histories on an infinite surface and the pressure relief waveforms are also plotted in Figure 6. These correspond to the LAMB and Hudson predictions, respectively. It should be noted that a single clearing wave originating from the horizontal free edge is shown, as the monitoring point is placed on the ground and therefore the vertical free edge clearing wave is ignored ($L_v >> L_H$).

A comparison of the EMBlast and CFD (BlastFoam) impulse predictions for above-ground explosions is presented in Table 2. A single scaled distance and height of 1.6 m/kg$^{1/3}$ and 0.6 m/kg$^{1/3}$, respectively, were considered. The EMBlast predictions are within 8% of the CFD impulse values, demonstrating that the Hudson clearing method can also be applied to above-ground explosions. Figure 7 compares the pressure-

time histories predicted by EMBlast with the BlastFoam results. Two successive positive peaks are observed in both the EMBlast predictions and the CFD results in Figure 7, indicating that incident and ground-reflected waves arrive separately at the target point. This demonstrates that the monitoring point at V_T = 0.6 m above the ground is in fact above the triple-point path, as predicted by UFC 3-340-02 and discussed in the previous section. However, the time of arrival of the ground-reflected wave predicted by EMBlast is faster compared to the CFD predictions. This is attributed to a modification to the LAMB addition implemented in EMBlast to improve agreement with CFD results.

Table 1. Comparison of the positive phase impulse values predicted by the EMBlast method with CFD analyses for free-air explosions.

		IMPULSE, I [kPa-msec]					
		CFD			EMBlast		
Reflecting surface type	**Distance of target point from free edge [mm]**	**Z = 0.8 m/kg$^{1/3}$**	**Z = 1 m/kg$^{1/3}$**	**Z = 1.6 m/kg$^{1/3}$**	**Z = 0.8 m/kg$^{1/3}$**	**Z = 1 m/kg$^{1/3}$**	**Z = 1.6 m/kg$^{1/3}$**
Infinite Surface	N/A	687.45*	522.88*	327.31	838.52	672.86	342.35
Finite Surface S = 200 mm	200	683.70*	522.20*	293.35	815.79	635.22	294.58
	100	N/A	N/A	277.89	753.45	574.56	267.33
Finite Surface S = 100 mm	100	620.00*	473.60*	251.89	753.45	574.56	267.33
	50	N/A	N/A	237.27	685.20	519.40	248.02

*Values derived from digitised pressure-time histories from Autodyn (Shin and Whittaker, 2019).

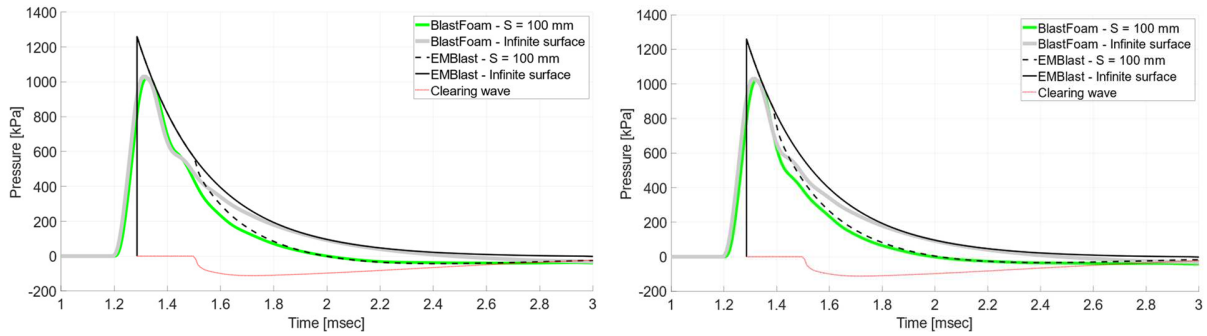

Figure 6. Comparison of the pressure-time histories derived with EMBlast and BlastFoam for a free-air explosion (Z = 1.6 m/kg$^{1/3}$) for a finite size target of half-width S = 100 mm: a) 100 mm away from the free edge, b) 50 mm away from the free edge.

Table 2. Comparison of the positive phase impulse values predicted by the EMBlast method with CFD analyses for an above-ground explosion (Z = 1.6 m/kg$^{1/3}$, V_E = 0.6 m and V_T = 0.6 m).

Reflecting surface type	Distance of target point from free edge [mm]	IMPULSE, I [kPa-msec]	
		CFD	EMBlast
Infinite Surface	N/A	593.85	551.61
Finite Surface S = 200 mm	200	482.67	462.56
	100	460.60	425.25
Finite Surface S = 100 mm	100	399.93	425.25
	50	381.50	395.57

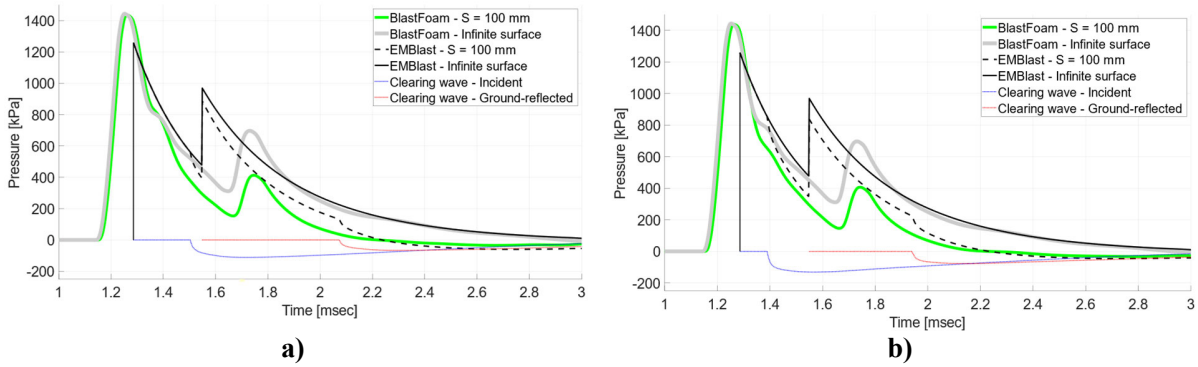

Figure 7. Comparison of the pressure-time histories derived with EMBlast and BlastFoam for an above-ground explosion (Z = 1.6 m/kg$^{1/3}$, V_E = 0.6 m and V_T = 0.6 m) for a finite size target of half-width S = 100mm: a) 100mm away from the free edge, b) 50mm away from the free edge.

CONCLUSIONS

This paper has assessed the application of the Hudson methodology to near-field blast loading and above-ground explosions. For the former, scaled distances greater than 0.8 m/kg$^{1/3}$ were considered. For the latter, the scope was limited to targets points located above the triple-point path, where the incident and ground-reflected waves arrive separately at the target. In both cases, the pressure relief clearing waves were obtained from Hudson's published graphs and the reflected pressure-time histories on infinite surfaces were derived from the semi-empirical Low Altitude Multiple Burst (LAMB) addition method. The positive phase impulse values predicted from the Hudson clearing method were compared with computational fluid dynamic analyses, demonstrating a good agreement for both the near-field blast loading and above-ground explosions. Future work will focus on developing fast-running models for near-field blast loading with scaled distances less than 0.8 m/kg$^{1/3}$. At these scaled distances, typically within the fireball radius, the shock front is less likely to be planar and semi-analytical methods, such as the Hudson method, are less likely to yield accurate predictions. Therefore, a machine learning approach will be considered by training artificial neural networks, using a combination of experimental and numerical data.

ACKNOWLEDGMENTS

The authors gratefully acknowledge Innovate UK for funding this research through a Knowledge Transfer Partnership (KTP).

REFERENCES

Angelides, S. C., Burgan, B.A., Kyprianou, C., Rigby, S.E., Tyas, A.: EMBlast: A software for rapidly and accurately predicting blast loads on structures. In: Proceedings of 97th Conference of the International Committee for Industrial Construction, Paphos (2022).

Hudson, C. C.: SC-TM-191-55-51: Sound pulse approximations to blast loading (with comments on transient drag). Sandia Corporation Technical Memorandum (1955). https://www.osti.gov/opennet/servlets/purl/16340913-1cPgoX/16340913.pdf

Kingery, C. N., Bulmash, G.: ARBRL-TR-02555: Airblast Parameters from TNT Spherical Air Burst and Hemispherical Surface Burst (1984).

Nartu, M. K., Kumar, M., Ramisetti, S. B.: Improved Methodology for Accurate Prediction of Blast Wave Clearing on a Finite Target. Journal of Engineering Mechanics, 148(9) (2022). https://doi.org/10.1061/(ASCE)EM.1943-7889.0002134

Rigby, S.E.: Blast Wave Clearing Effects on Finite-Sized Targets Subjected to Explosive Loads. Ph.D. Dissertation. University of Sheffield, Sheffield (2014).

Rigby, S. E., Tyas, A., Clarke, S. D., Fay, S. D., Reay, J. J., Warren, J. A., Pope, D. J.: A Review of UFC-3-340-02 Blast Wave Clearing Predictions. In: Proceedings of 16th International Symposium for the Interaction of the Effects of Munitions with Structures, Destin (2015a).

Rigby, S.E., Tyas, A., Clarke, S.D., Fay, S.D., Reay, J. J., Warren, J. A., Gant, M., Elgy, I.: Observations from Preliminary Experiments on Spatial and Temporal Pressure Measurements from Near-Field Free Air Explosions. International Journal of Protective Structures, 6(2), 175-190 (2015b). https://doi:10.1260/2041-4196.6.2.175

Shin, J., Whittaker, A. S.: Blast-Wave Clearing for Detonations of High Explosives. Journal of Structural Engineering, 145(7) (2019). https://doi.org/10.1061/(ASCE)ST.1943-541X.0002327

Tyas, A., Warren, J. A., Bennett, T., Fay, S.: Prediction of clearing effects in far-field blast loading of finite targets. Shock Waves, 21, 111–119 (2011). https://doi.org/10.1007/s00193-011-0308-0

UFC 3-340-01: Design and Analysis of Hardened Structures to Conventional Weapons Effects. US Army Corps of Engineers (2002).

UFC 3-340-02: Structures to Resist the Effects of Accidental Explosives. US Army Corps of Engineers (2014).